[Supplementary material]

Between foraging and farming: strategic responses to the Holocene Thermal Maximum in Southeast Asia

Marc F. Oxenham[1], Hiep Hoang Trinh[2], Anna Willis[3], Rebecca K. Jones[1], Kathryn Domett[4], Cristina Castillo[5], Rachel Wood[1], Peter Bellwood[1], Monica Tromp[6], Ainslee Kells[1], Philip Piper[1], Son Thanh Pham[7], Hirofumi Matsumura[8] & Hallie Buckley[9]

[1] *School of Archaeology & Anthropology, A.D. Hope Building, Australian National University, 14 Ellery Crescent, Acton ACT 2601, Australia*

[2] *Department of Prehistoric Archaeology, Vietnam Institute of Archaeology, 61 Phan Chu Trinh, Hoan Kiem, Hanoi, Vietnam*

[3] *College of Arts, Society & Education, James Cook University, Townsville, Qld 4811, Australia*

[4] *College of Medicine & Dentistry, James Cook University, Townsville, Australia*

[5] *Institute of Archaeology, University College London, 31–34 Gordon Square, London WC1H 0PY, UK*

[6] *Department of Archaeology, Max Planck Institute for the Science of Human History, Kahlaische Strasse 10, D-07745, Jena, Germany*

[7] *Department of Life Sciences and Biotechnology, Ferrara University, Via L. Borsari, 46-44121 Ferrara, Italy*

[8] *School of Health Science, Sapporo Medical University, S1W17, Chuoh-ku Sapporo, Hokkaido 060-8556, Japan*

[9] *Department of Anatomy, University of Otago, P.O. Box 56, Dunedin 9054, New Zealand*

[*] *Author for correspondence (Email: marc.oxenham@anu.edu.au)*

Received: 8 June 2017; Accepted: 12 September 2017; Revised: 26 September 2017

SI. Radiometric dating

Radiocarbon dating at CCN was exceptionally challenging given the poor preservation of protein. At the Australian National University, 11 bones/dentine were screened for nitrogen content. This provides an indication of whether protein, the major source of nitrogen in bone, is preserved (Brock et al. 2012). If the bone is more than 0.7% nitrogen there is a c.70% chance that enough collagen remains for radiocarbon dating. Unfortunately, the %N at CCN ranged between 0.01 and 0.04, far below this cut off. As collagen is not preserved at CCN,

carbonate in tooth enamel was dated to obtain a *minimum age* for the burials and faunal remains in the surrounding midden, alongside calcined antler to ascertain the age of an unusual and apparently structured deposit over burial M133. A charred *Canarium* seed was also dated that was recovered between 20 and 30cm below the top of the midden or burial layer (context or layer 2). This sample material provides an accurate date. However, it is not a direct date on the burials, although within the burial layer, and may be affected by the mixture of deposits through the site.

Enamel and calcined bone are less porous and contain larger and more stable hydroxyapatite crystals than unburnt bone and dentine. However, all ages on these materials from Con Co Ngur are likely to be erroneously young. It is well known that radiocarbon dates on tooth enamel underestimate the true age of samples (Hedges et al. 1995, Grün et al. 1997, Zazzo 2014) as the pretreatment routinely applied does not remove all carbonate contaminants from the groundwater, most likely located in nanometer-sized pores in the structure (Wood et al. 2016). Calcined bone has been used to date cremated bone from the mid-Holocene age in northern Europe and, if an old-wood effect is taken into account, is often thought to give reliable age estimates (Lanting et al. 2001, Olsen et al. 2008, Zazzo et al. 2013). However, even in temperate environments, calcined bone can give erroneously young ages (van Strydonck et al. 2009). Thus, calcined bone can be affected by diagenetic processes which are likely to be accelerated in hot and wet environments. Until further testing on known aged samples is carried out on material from such environments, ages should be considered potentially affected by diagenetic processes and thus be minimum age estimates.

A dremel drill was used to remove the dentine and exterior surface from the enamel and to clean soft material from any cracks prior to grinding to a fine powder in an agate pestle and mortar under ultrapure water and treating with acetic acid under a weak vacuum (1M/ 10-24 hours/ room temperature). In an attempt to improve the age estimate of the samples, two acid leach protocols were applied to two Bovid teeth (13CCN-407 and 13CCN-082). The first followed the protocol used for all samples in this study, using 1ml 1M acetic acid for every 50mg enamel. The second used twice the concentration of acid.

Before preparation for radiocarbon dating, FTIR spectroscopy was used to check the crystallinity of calcined antler. When calcined the splitting factor, a measure of the order of the phosphate crystals, increases to around 7 (Olsen et al. 2008). Two antler fragments contained areas with a crystallinity index close to 7 and were treated for radiocarbon dating. 13CCN-951-2 had a blue-grey core with a splitting factor of 6.5 whilst 13CCN-949-950 had a white outer layer with a splitting factor of 6.9. After physical cleaning to remove the

surface, white or blue-grey calcined material was removed with a drill, samples were soaked in 1.5% sodium chlorite bleach (pH3, 48 hours, c.10ml), rinsed in ultrapure water and treated with acetic acid following the method described for tooth enamel.

The charred *Canarium* seed was pre-treated using an acid-base-acid protocol. This involved HCl (1M, 70^{o}C, 30 minutes), NaOH (1M, 70^{o}C, 1 hour, solution replaced until colourless) and HCl (1M, 70^{o}C, 30 minutes), rinsing with ultrapure water between treatments.

Cleaned and rinsed enamel and calcined antler were freeze-dried, reacted with 85% phosphoric acid at 80^{o}C in an evacuated Vacutainer^{TM}. The charred seed was combusted in a sealed quartz tube with CuO wire and Ag foil. The CO_2 generated from both methods was cryogenically collected and purified before graphitisation over an iron catalyst in the presence of hydrogen. Graphite targets were measured in a single stage NEC AMS at the Australian National University (Fallon et al. 2010). Dates have been calculated according to Stuiver & Polach (1977) and corrected using a $\delta^{13}C$ value measured by AMS.

Most of the results fall between c.6700 – 6200 cal BP, although the antler and one *Bubalus* tooth (SANU-41038) are younger ranging between c.6200 – 5700 cal BP. With the exception of one sample (SANU-41036) all teeth contain around 0.7 %C and all antler around 0.3 %C, as is typical for these materials. When 13CCN-407 was dated twice using the same methods (SANU-41037, 41107) the dates are indistinguishable at 95.4% according to a Chi squared test (T=1.7; df 1, 5% 3.8). Similarly the teeth dated with both the routine and more aggressive acid pretreatment yielded indistinguishable ages (T=0.0 for 13CCN-516 and T=1.9 for 13CCN-082; df 1, 5% 3.8). The reasonable carbon contents and excellent reproducibility do not indicate that the results are accurate. %C is a relatively coarse measure of potential additional carbon. Wood, et al. (2016) has shown carbonate contaminants probably sit between the apatite crystallites in tooth enamel, and are inaccessible to the acid. This means that additional leaching is unlikely to improve the age estimate.

It must be stressed that these dates most likely represent minimum age estimates. Each sample may be affected by a different amount of contamination, so it is impossible to establish how long the cemetery and midden may have been in use. The young dates on the two calcined antlers, found in close proximity to burial M133, are particularly pronounced. Not only are the two dates inconsistent with each other, but they are nearly 1000 years younger than a date on enamel from burial M133. Known age calcined bone has not been dated from tropical environments, and the likelihood of diagenetic alteration is not clear. This work suggests alteration may be extensive.

One further factor to consider, given the presence of freshwater, estuarine and marine aquatic species present at the site, is the potential that the dates on human enamel are affected by a radiocarbon reservoir effect. This would make the dates appear older than they are when calibrated against the atmospheric calibration curve. However, it is unlikely that this is currently a significant problem as the dates on human teeth overlap in range with those on herbivorous faunal tooth enamel. If a radiocarbon reservoir is present, it appears to be overprinted by problems relating to diagenesis and contamination by young carbon.
The charred *Canarium* seed is older than all but one date on enamel, suggesting some use of the site in the early 7th millennium. Given the mixed nature of the midden deposit, it is not clear how well associated this seed is with the burials. It does, however, support the hypothesis that the dates on enamel and calcined bone are likely to be too young.

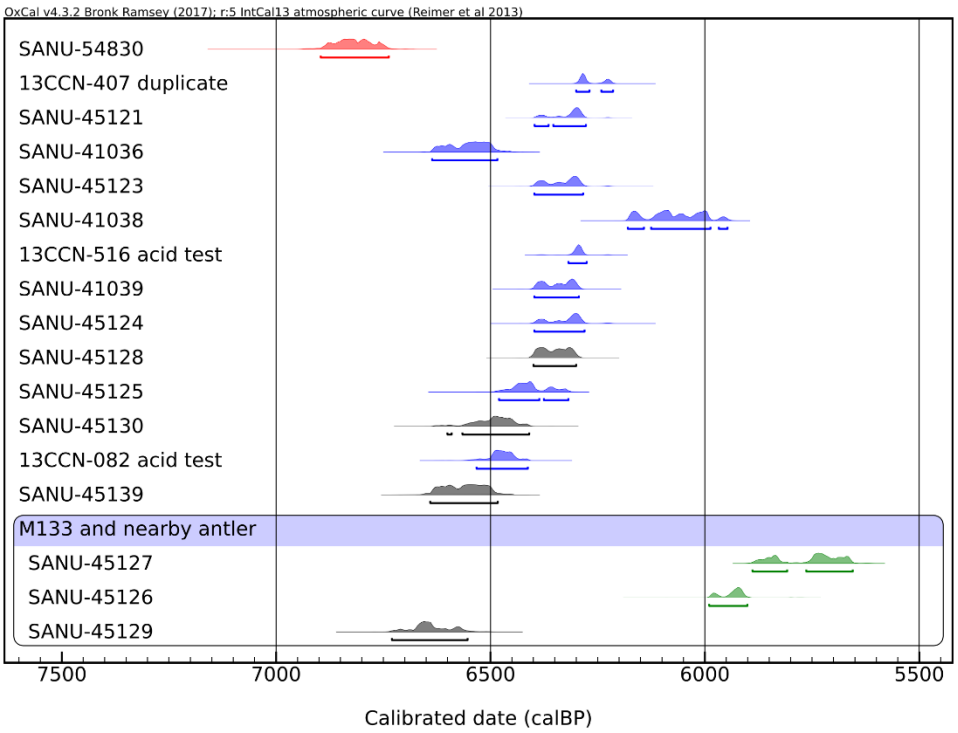

Figure S1; Radiocarbon dates on charred *Canarium* seed (red), calcined antler (green), human tooth enamel (grey) and faunal tooth enamel (blue). All except the seed are likely to be minimum age estimates. Samples have been calibrated against IntCal13 (Reimer et al. 2013) in OxCal c.4.2 (Ramsey 2009). Where two dates were undertaken on a single sample a chi squared test was undertaken to ensure the ages were indistinguishable at 95.4% probability, and the weighted average calculated.

Table S1. Radiocarbon ages from Con Co Ngua. Samples have been calibrated against IntCal13 (Reimer et al. 2013) in OxCal c.4.2 (Ramsey 2009). Where two dates were undertaken on a single sample a chi squared test was undertaken to ensure the ages were indistinguishable at 95.4% probability, and the weighted average calculated.

ID	SANU-	CONTEXT	SAMPLE	MATERIAL	$\delta^{13}C$[3]	%C[4]	^{14}C age (BP)	±	cal BP (95.4% range)
13CCN-407	41037	LII M75	*Bubalus*, L molar	Enamel	-4.6	0.7	5440	25	6300-6214
	41107[1]				-2.6	0.8	5485	24	
13CCN-1918	45121	LII.4 g2-3	Bovinae, LI2, R	Enamel	-6.7	0.7	5514	28	6397-6278
13CCN-062	41036	LII.4 b,c,d	*Cervus/Rusa*, UM3, L	Enamel	-5.5	2.2	5750	25	6636-6484
13CCN-1216	45123	LIII.1 b12	Bovinae, L molar	Enamel	-6.7	0.7	5528	32	6398-6284
13CCN-408	41038	LIII.2	*Bubalus*, L molar	Enamel	-11.5	0.7	5280	25	6180-5947
13CCN-516	43330	LIII.2	*Bubalus*, UP1, R	Enamel	-1.5	0.8	5497	25	6318-6276
	43331[2]				-2.5	0.7	5502	26	
13CCN-409	41039	LIII.4	Bovinae, LM3, L	Enamel	-3.8	0.8	5545	25	6398-6294
13CCN-1079	45124	M136	Bovinae, L molar	Enamel	-2.6	0.7	5521	31	6398-6281
	45128	M21	Human, LM3	Enamel	-18.0	0.8	5560	27	6400-6300
13CCN-1222	45125	under M17	Bovinae, UP3, R	Enamel	-4.1	0.8	5631	28	6480-6319

	45130	M11	Human, LM3	Enamel	-17.6	0.8	5708	28	6601-6410
13CCN-082	43329	M55	*Bubalus*, LM1, R	Enamel	-2.9	0.7	5673	26	6533-6413
	43332[2]				-2.7	0.7	5724	26	
13CCN M142 RM3	45139	M142	Human RM3?	Enamel	-17.1	0.8	5758	28	6641-6483
13CCN-951-2	45127	close to M133, F43, E6-7	Muntjac, antler	Calcined antler	-17.4	0.3	5008	29	5889-5655
13CCN-949-950	45126	close to M133, F43, E6-7	*Cervus*, antler	Calcined antler	-19.6	0.3	5172	27	5990-5901
CCNH1 L2.3 E10	54830		*Canarium* sp.	Charred seed	-26		5982	30	6896 – 6737
	45129	M133	Human, LM3	Enamel	-17.8	0.7	5828	29	6730-6554

1. The sample was dated using the same preparation protocol a second time to assess reproducibility.

2. The sample treated with a more rigorous acid leach prior to dating.

3. $\delta^{13}C$ was measured on an AMS and is not equivalent to IRMS measurements

4. %C was measured volumentrically and is not as precise as IRMS measurements

References

BROCK, F., R. WOOD, T.F.G. HIGHAM, P. DITCHFIELD, A. BAYLISS & C. BRONK RAMSEY. 2012. Reliability of Nitrogen Content (%N) and Carbon:Nitrogen Atomic Ratios (C:N) as Indicators of Collagen Preservation Suitable for Radiocarbon Dating. *Radiocarbon* 54: 879-886. https://doi.org/10.1017/S0033822200047524

FALLON, S.J., L.K. FIFIELD & J.M. CHAPPELL. 2010. The Next Chapter in Radiocarbon Dating at the Australian National University: Status Report on the Single Stage Ams. *Nuclear Instruments and Methods in Physics Research Section B: Beam Interactions with Materials and Atoms* 268: 898-901. https://doi.org/10.1016/j.nimb.2009.10.059

GRÜN, R., M. ABEYRATNE, J. HEAD, C. TUNIZ & R.E.M. HEDGES. 1997. Ams ^{14}c Analysis of Teeth from Archaeological Sites Showing Anomalous Esr Dating Results. *Quaternary Science Reviews* 16: 437-444. https://doi.org/10.1016/S0277-3791(96)00093-5

HEDGES, R.E.M., J.A. LEE-THORP & N.C. TUROSS. 1995. Is Tooth Enamel Carbonate a Suitable Material for Radiocarbon Dating? *Radiocarbon* 37: 285-290. https://doi.org/10.1017/S0033822200030757

LANTING, J.N., A.T. AERTS-BIJMA & J. VAN DER PLICHT. 2001. Dating of Cremated Bones. *Radiocarbon* 43: 249-254. https://doi.org/10.1017/S0033822200038078

OLSEN, J., J. HEINEMEIER, P. BENNIKE, C. KRAUSE, K. MARGRETHE HORNSTRUP & H. THRANE. 2008. Characterisation and Blind Testing of Radiocarbon Dating of Cremated Bone. *Journal of Archaeological Science* 35: 791-800. https://doi.org/10.1016/j.jas.2007.06.011

RAMSEY, C.B. 2009. Bayesian Analysis of Radiocarbon Dates. *Radiocarbon* 51: 337-360. https://doi.org/10.1017/S0033822200033865

REIMER, P.J., E. BARD, A. BAYLISS, J.W. BECK, P.G. BLACKWELL, C. BRONK RAMSEY, P.M. GROOTES, T.P. GUILDERSON, H. HAFLIDASON, I. HAJDAS, C. HATTÉ, T.J. HEATON, D.L. HOFFMANN, A.G. HOGG, K.A. HUGHEN, K.F. KAISER, B. KROMER, S.W. MANNING, M. NIU, R.W. REIMER, D.A. RICHARDS, E.M. SCOTT, J.R. SOUTHON, R.A. STAFF, C.S.M. TURNEY & J. VAN DER PLICHT. 2013. Intcal13 and Marine13 Radiocarbon Age Calibration Curves 0–50,000 Years Cal Bp. *Radiocarbon* 55: 1869-1887. https://doi.org/10.2458/azu_js_rc.55.16947

STUIVER, M. & H.A. POLACH. 1977. Discussion Reporting of 14c Data. *Radiocarbon* 19: 355-363. https://doi.org/10.1017/S0033822200003672

VAN STRYDONCK, M., M. BOUDIN & G. DE MULDER. 2009. 14c Dating of Cremated Bones: The Issue of Sample Contamination. *Radiocarbon* 51: 553-568. https://doi.org/10.1017/S0033822200055922

WOOD, R., M. DUVAL, N.T. MAI HUONG, N.A. TUAN, A.-M. BACON, F. DEMETER, P. DURINGER, M. OXENHAM & P. PIPER. 2016. The Effect of Grain Size on Carbonate Contaminant Removal from Tooth Enamel: Towards an Improved Pretreatment for Radiocarbon Dating. *Quaternary Geochronology* 36: 174-187. https://doi.org/10.1016/j.quageo.2016.08.010

ZAZZO, A. 2014. Bone and Enamel Carbonate Diagenesis: A Radiocarbon Prospective. *Palaeogeography, Palaeoclimatology, Palaeoecology* 416: 168-178. https://doi.org/10.1016/j.palaeo.2014.05.006

ZAZZO, A., M. LEBON, L. CHIOTTI, C. COMBY, E. DELQUÉ-KOLIČ, R. NESPOULET & I. REICHE. 2013. Can We Use Calcined Bones for 14c Dating the Paleolithic? *Radiocarbon* 55: 1409-1421. https://doi.org/10.1017/S0033822200048347

Table S2. Complete taxonomic list of species identified in the CCN faunal assemblage.

Class	Order	Family	Taxon	Common Name	NISP
Crustacea					
(Subphylum)				Crabs, lobsters, crayfish	4
Elasmobranchii				Sharks and rays	28
(Subclass)[1]	Selachimorpha				
	(Superorder)			Sharks	1
	cf. Lamniformes			Mackerel sharks	3
	cf. Orectolobiformes			Carpet sharks	1
	cf. Carcharhiniformes			Ground sharks	7
	Myliobatiformes			Rays	7
Teleostei				Bony fishes	451
(Infraclass)	Siluriformes			Catfish	4
	Perciformes			Perch-like fishes	7
		Serranidae		Basses, groupers	4
		Sparidae		Breams, porgies	4
		Scaridae		Parrotfish	1
	Tetraodontiformes			Ray-finned fishes	1
Reptilia				Reptiles	17
	Testudines			Turtles	119
		Geoemydidae		Hard-shell turtles	393
			cf. *Cyclemys dentata*	Asian leaf turtle	5
			cf. *Siebenrockiella crassicollis*	Black marsh turtle	1

[1] The taxonomic order of Elasmobranchii frequently changes, this is based on (Vélez-Zuazo and Agnarsson 2011).

		Trionychidae		Soft-shell turtles	40
	Squamata			Lizards and snakes	6
		Varanidae	*Varanus* spp.	Monitor lizard	30
	Serpentes (Suborder)			Snakes	24
Aves				Birds	20
	Galliformes	cf. Phasianidae		Pheasants, fowls	2
	Ciconiiformes	Ciconiidae	*Leptoptilos dubius*	Greater adjutant	2
		cf. Ciconiidae		Storks	1
	Pelecaniformes	cf. Ardeidae		Herons	5
Mammalia					3539
		Muridae	cf. *Rattus* spp.	Rats, mice	7
		Hystricidae		Porcupine	2
			Hystrix brachyura	Malayan Porcupine	1
	Rodentia		cf. *Atherurus macrourus*	Asiatic brush-tailed porcupine	1
		Sciuridae		Squirrels	2
			Small rodent		2
			Large rodent		2
		Cercopithecidae		Old World monkeys	2
	Primates		*Macaca* spp.	Macaque	4
			cf. *Macaca* spp.		2
			Trachypithecus	Leaf monkey	1
	Pholidota	Manidae	*Manis* spp.	Pangolin	5
	Carnivora				22

	Felidae			1
		Panthera cf. *tigris*	Tiger[2]	3
		cf. *Neofelis or Pardofelis*	Clouded leopard or marbled cat	7
	Viverridae		Civet cats	3
		cf. *Viverra*		3
		Viverra spp.	Large Indian civet, large spotted civet	1
	Canidae		Jackals, wolves, dhole, foxes	2
		Cuon alpinus	Dhole/Asian wild dog	1
	Mustelidae	Lutrinae	Otters	1
		Aonyx cinereus	Oriental small-clawed otter	5
	Phocidae		Seal	1
				22
	Suidae	*Sus* cf. *scrofa*	Eurasian wild boar	50
	Pecora		cf. Bovinae or Cervidae	16
Artiodactyla	Cervidae		Deer	113
		Cervus/Rusa spp.	Deer	99
		Muntiacus spp.	Muntjac	9
		Small cervid		50

[2] These elements were identified as tiger because of their large size, though it is possible they could be panther. Unfortunately, it is difficult to differentiate between members of the family Felidae as they are morphologically similar and distinction is mainly based on size and geographical boundaries.

		Medium-large cervid		27
	Bovinae		Cattle, water buffalo	236
		Bubalus sp.	Water buffalo	96
		cf. *Bubalus*		30
		Bos spp.	Cattle	6
		cf. *Bos*		10
Cetacea			Whale	1
Unidentified				3972
Total				**9545**

Table S3. Summary of artefacts and anthropogenically modified skeletal elements in CCN assemblage.

ID	Context	Taxon	Element	Anth modified	Description
2828	LI.2	UNID		Artefact	Shaped and rounded into a point. Surface appears polished.
65	LII.4 B,C,D1	Mammal large	Long bone shaft	Artefact	Shaft has been rounded at both ends and abrasion/use wear marks are visible at both ends. Polish on both surfaces.
2529	LII M77	UNID	Shaft fragment	Artefact	Similar to 065 but smaller
1843	LII.4 D10	Mammal	Long bone shaft	Artefact	Similar to 065 but smaller. Heavy Mn staining makes it difficult to see abrasion/use wear
1774	LII.1 F29	Medium mammal cf. Cervidae	Long bone cf. metapodial	Artefact	Shaft is split in half longitudinally and rounded and polished on edges. Distal end comes to a narrow point. Abrasions marks visible on surface
2865	LII.1 F26	Cervidae	Distal metapodial	Artefact	Similar to 1774
2866	LII.1 F26	Cervidae	Metapodial, shaft	Artefact	Attaches to 2865
2168	LII.4 M34	Cervidae cf. *Rusa*	Distal metacarpal	Artefact	Similar to 1774
2493	M53/54	Cervidae cf. *Rusa*	Left proximal metacarpal	Artefact	Similar to 1774
2749	LII.1 F26	Cervidae	Antler fragment	Artefact	Rounded, deep longitudinal grooves marks on surface, also smaller transverse and oblique marks
1779	M74	UNID Aves?	Long bone shaft	Artefact	Shaped and rounded along the shaft. The pointed end of the shaft has been shaped so there is a V projecting into the shaft, this end was also broken in

					antiquity. No sign of retouch after the end was broken.
2241	M22/23	UNID Mammal?		Artefact	Deliberately shaped into a roughly rectangular shape and rounded along edges. Bone is very thin. In two pieces.
2259	M22/23	*Sus* cf. *scrofa*	Lower left canine	Artefact	Inner surface has transverse abrasion marks and towards the root end there is a slight notch/groove.
2403	M92	*Leptoptilos dubius*	Proximal tarsometatarsus	Artefact	Abrasions marks and rounding along the shaft
2455	LII M66	Cervidae	Distal metapodial	Modified	Chopped through centre of condyle, small grooves
3135	LII.1 F29	Cervidae	Proximal metapodial	Modified	Probably similar technique to 1774, missing distal shaft
3209	LII.1 F9 B7	UNID		Modified	Abrasion/use wear marks visible
3188	LII.2	UNID		Modified	Clear groove marks on surface
2459	M6	Mammal medium-large	Long bone shaft	Modified	Two parallel grooves running longitudinal to shaft, possible artefact debitage

S4. Burial practices inferred through field anthropology

The mortuary practices at Cồn Cổ Ngựa were interpreted using *L'Anthropologie de terrain* or Field anthropology, a method which uses archaeological, osteological and taphonomic observations to understand and interpret the context in which individuals were interred as part of their associated mortuary practices (Duday et al. 1990, Nilsson 1998, Pautreau et al. 2004, Duday 2006, Duday & Guillon 2006, Nilsson Stutz 2006, Nilsson Stutz et al. 2008, Willis & Tayles 2009, Harris & Tayles 2012). It is a method which assesses each skeletal element and the relationship of them to one another, to understand how the elements of a human skeleton move as associated soft tissues decompose with an aim to conceptualise the original position of the individual, to assist in understanding the context in which the individual was interred. The most reliable evidence for a primary burial is the maintenance of the articulation of labile joints and the anatomical congruence of contiguous bones. Labile joints are those that have the least amount of associated fibrous tissue or ligaments and therefore disarticulate the fastest; they include the bones of the hand and phalanges of the feet, the cervical vertebrae and the scapulo-thoracic joint. Persistent joints are those that have the most associated fibrous tissue and ligaments as a function of the biomechanical stress they endure and therefore disarticulate slower; for example, the atlanto-occipital articulation, the articulations of the lumbar vertebrae, the lumbo-sacral joint, the sacroiliac joint, the knees and the tarsals. The movement of the skeletal elements as an individual decomposes are dictated by two further factors, gravity and the spaces created by soft tissue decomposition. While the amount of movement is influenced by the context or container in which the individual was interred (Duday et al. 1990, Nilsson 1998, Pautreau et al. 2004, Duday 2006, Duday & Guillon 2006, Nilsson Stutz 2006, Nilsson Stutz et al. 2008, Willis & Tayles 2009, Harris & Tayles 2012). There was some variation observed in the mortuary practices at Cồn Cổ Ngựa with individuals interred in two burial positions, squatting and side flexed in a foetal position. The individuals who were interred in a squatting position were all primary interments; indicated by the maintenance of anatomically contiguous joints and labile joints. The classic squatting position was lower limbs flexed, hyperflexed at the hips and knees, while upper limbs were generally crossed in the abdominal area, the forearms either pronated or supinated. The movement of skeletal elements was a reflection of gravity, the secondary spaces created during soft tissue decomposition and the context in which they were interred. The majority of the femora, tibiae, fibulae and humeri maintained their stable position, while the smaller elements and labile joints in unstable positions moved, except for the feet which maintained anatomical integrity because they were stabilised at the base of the grave. There was

movement observed among smaller elements of the labile joints, including the cervical vertebrae, the scapula-thoracic joints and the patellae for example, this indicates that soil did not continuously replace the soft tissues as they decomposed and with nothing to stabilise them in their unstable positions they moved. Constriction affects were also observed around the distal phalanges of the feet, which were often at a right angle and restricted within the limit of the pit. These observations are consistent with the individuals being wrapped before burial in a semidurable material. While most of the squatting burials were interred in small pits with a narrow diameter there was a range of positional variation among the squatting burials, some had fallen to either the left or right side, forwards or backwards. Despite this they maintained their anatomical squatting position as they moved, providing further evidence that they were wrapped and moved as a unit. However, there must have been secondary spaces created within these pits to allow this to occur. One possibility is that there were organic grave goods in these pits, for example, woven baskets interred adjacent to the individuals which created secondary spaces in which the individuals moved into during decomposition. There was also a large amount of variation in the position of the skulls, which migrated as a function of gravity into the abdominal area with the reduction and compaction of this area creating secondary spaces. This was in some cases not sufficient to explain the positional variation however.

The individuals who were interred side flexed in a foetal position also represented primary interments. They were either lying on their right or left sides, with their lower limbs flexed, either hyperflexed or loosely flexed at the hip with their knees flexed and their upper limbs flexed, either pronated or supinated with their hands placed near the mandible. The subtle movement and constriction of skeletal elements within the limits of the grave are consistent with the individuals being wrapped. Further, the superposition of several individuals over one another in very close proximity, whilst maintaining anatomical integrity, indicates that they were separated in some way. The movement of labile joints and the overall maintenance of the anatomical position indicates that the wrapping would have been semidurable. Given the antiquity of the site, it is likely that the semidurable wrapping was bark cloth. At least six sites, the earliest dated to c.7900 cal BP, provide evidence for bark cloth beaters in Guangxi Province, southern China (Li et al. 2014). While bark cloth beaters have not been recovered from Da But contexts, the demonstrated interaction between hunter-gatherer communities in northern Vietnam and southern China during the mid-Holocene is suggestive of the technology being employed in Da But culture sites.

During the post excavation assessment of the human remains peri-mortem (assumed post-mortem) cut and chopping marks were observed on the shafts of the long bones (humerus, tibia and femur) and the clavicles of 58% of adults (50.0% females, 65.4% males), while head removal and repositioning occurred on occasion. This form of mutilation rises to 70% of all adults if incomplete or poorly preserved remains are included. One child (c. 7 years old) and 50% of >15 <19-year-old subadults were also treated in this manner. Chopping forces were sufficient to remove large flakes of cortical bone, which sometimes remained in situ. It is hypothesised that these may have been part of some postmortem manipulation and mutilation of the individuals, presumably related to community belief systems regarding death. It is also possible that the skulls were also removed due to the range of positional variation of the skulls, sometimes in inexplicable positions. At this stage this has not been investigated. It is likely that these rituals were undertaken before the individuals were placed into a squatting position and wrapped before being interred.

References

Duday, H. 2006. L'archeothanatologie Ou L'archeologie De La Mort (Archaeothanatology or the Archaeology of Death), in R. Gowland & C. Knusel (ed.) *Social Archaeology of Funerary Remains*: 30-56. Oxford: Oxbow Books.

Duday, H., P. Courtaud, E. Crubezy, P. Sellier & A.-M. Tillier. 1990. L' Anthropologie "De Terrain": Reconnaissance Et Interpretation Des Gestes Funeraires. *Bulletins et Memoires de la Societe d'Anthropologie de Paris* 2: 29-50. https://doi.org/10.3406/bmsap.1990.1740

Duday, H. & M. Guillon. 2006. Understanding the Circumstances of Decomposition When the Body Is Skeletonized, in A. Schmitt, E. Cunha & J. Pinheiro (ed.) *Forensic Anthropology and Medicine: Complementary Sciences from Recovery to Cause of Death*: 117-157. New Jersey: Humana Press.

Harris, N.J. & N. Tayles. 2012. Burial Containers – a Hidden Aspect of Mortuary Practices: Archaeothanatology at Ban Non Wat, Thailand. *Journal Of Anthropological Archaeology* 31: 227-239. https://doi.org/10.1016/j.jaa.2012.01.001

Li, D., Wang, W., Tian, F., Liao, W. and Bae, C.J., 2014. The oldest bark cloth beater in southern China (Dingmo, Bubing basin, Guangxi). *Quaternary International*, *354*, pp.184-189. https://doi.org/10.1016/j.quaint.2014.06.062

Nilsson, L. 1998. Dynamic Cadavers. *A field-anthropological analysis of the Skateholm II burials. Lund Archaeological Review*: 5-17.

Nilsson Stutz, L. 2006. Unwrapping the Dead: Searching for Evidence of Wrappings in the Mortuary Practices at Zvenjnieki, in L. Larsson & I. Zagorska (ed.) *Back to the Origin. New Research in the Mesolithic-Neolithic Zvejnieki Cemetery and Environment, Northern Latvia.*: 217-233.

Nilsson Stutz, L., L. Larsson & I. Zagorska. 2008. More Burials at Zvejnieki. Preliminary Results from the 2007 Excavation. *Mesolithic Miscellany* 19: 12-16.

Pautreau, J.-P., P. Mornais & T. Doy-Asa. 2004. *Ban Wang Hai : Excavations of an Iron-Age Cemetery in Northern Thailand*.). Chiang Mai Chesham: Silkworm; Combined Academic.

Willis, A. & N. Tayles. 2009. Field Anthropology: Application to Burial Contexts in Prehistoric Southeast Asia. *Journal of Archaeological Science* 36: 547-554. https://doi.org/10.1016/j.jas.2008.10.010

S5. CCN Characterisation of calcified cyst found with M59: Old Male

Fragments of an ellipsoid calcified object were found amongst the remains of Burial M59 post-excavation, in the bag of the pelvic bones. The object is smooth and light brown on the outer surface and the inner surface is chalky and white with a roughened surface. Due to its fragmentation, it is not possible to estimate the size of the complete object but one fragment which may be the end of the ellipse is no more than 2cm in diameter and the walls range in thickness from 1mm – 3mm (Figure S5.1).

Macroscopic appearance and light microscopy

Images of the probable cyst were taken at various magnifications using an Olympus SZX7 stereo microscope (Department of Archaeology and Anthropology), a Zeiss Sigma VP FEG SEM and a JEOL 6700F FE-SEM (Otago Centre for Electron Microscopy).

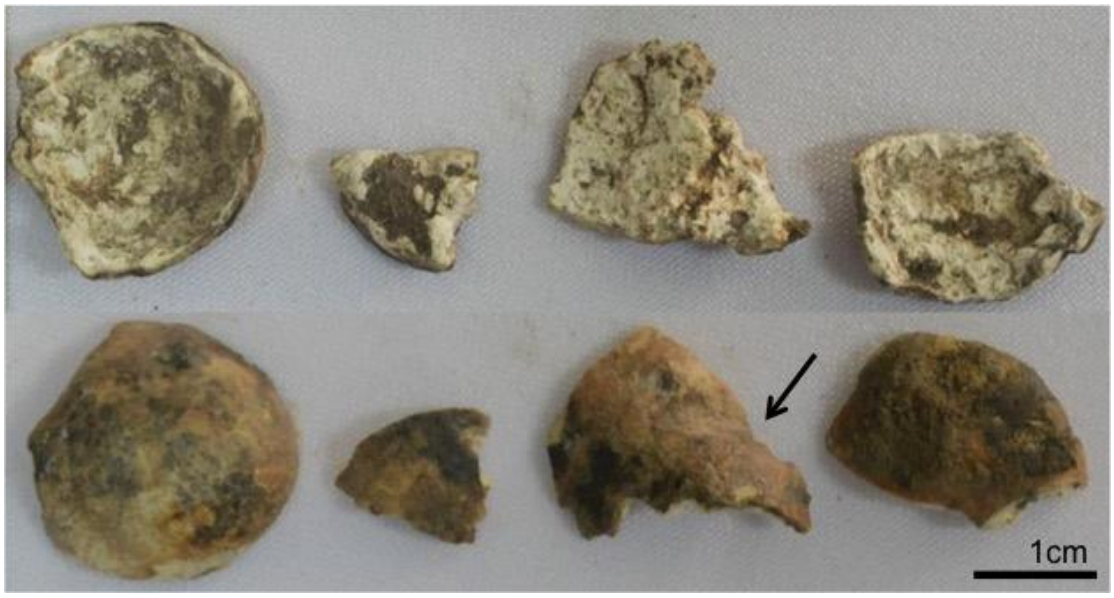

Figure S5.1. Inner surface of probable cyst (top). Outer surface of probable cyst (bottom). Arrow is pointing to saddle/shoulder that might show where a daughter cyst was forming.

The outside of the object is smooth and dense to the naked eye but low powered light microscopy reveals an irregular latticing is visible (Figures S5.1 and S5.2). The inner surface is highly irregular, friable and chalky in appearance (Figure S5.3). These morphological features of the object suggest is a calcified cyst and light microscopy also shows at least two distinct layers in the calcified wall (Figure S5.4).

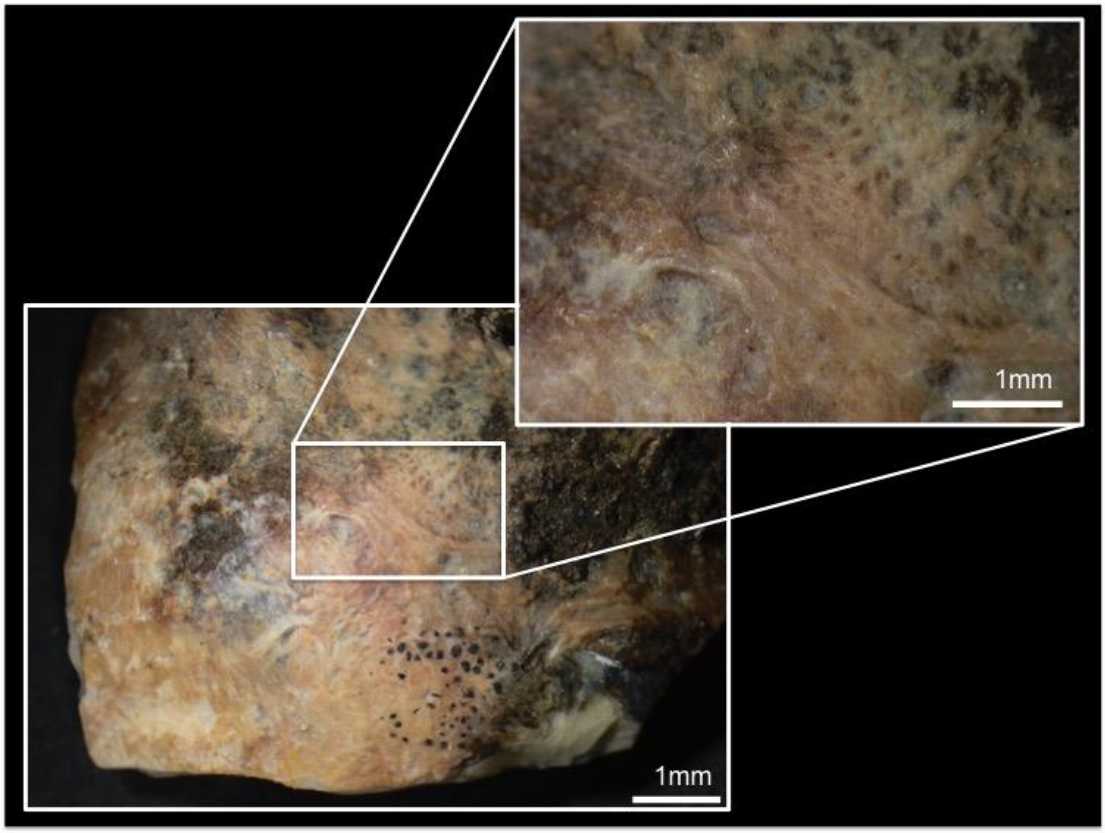

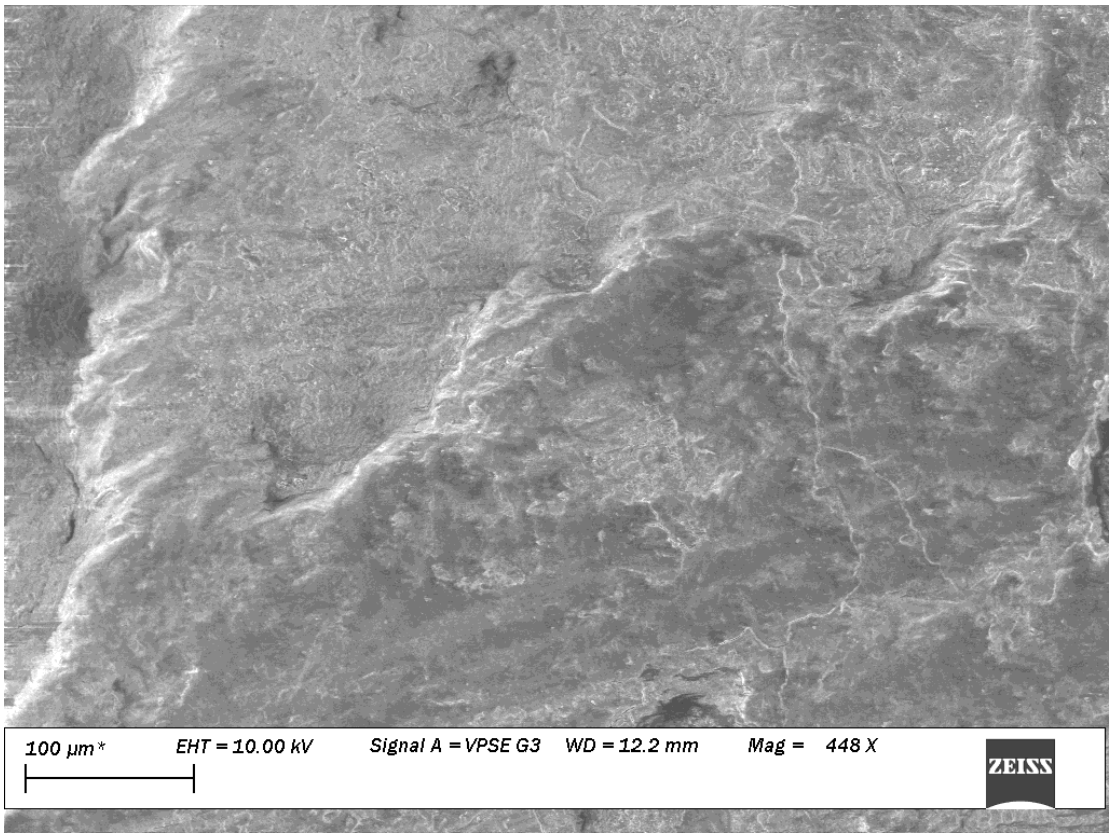

Figure S5.2. The outer surface of the probable cyst when seen with the naked eye, appears very smooth. However, when seen under low powered microscopy (top) a very fine and

highly irregular latticing is visible. When seen under SEM, it is clear that the surface is irregular (bottom).

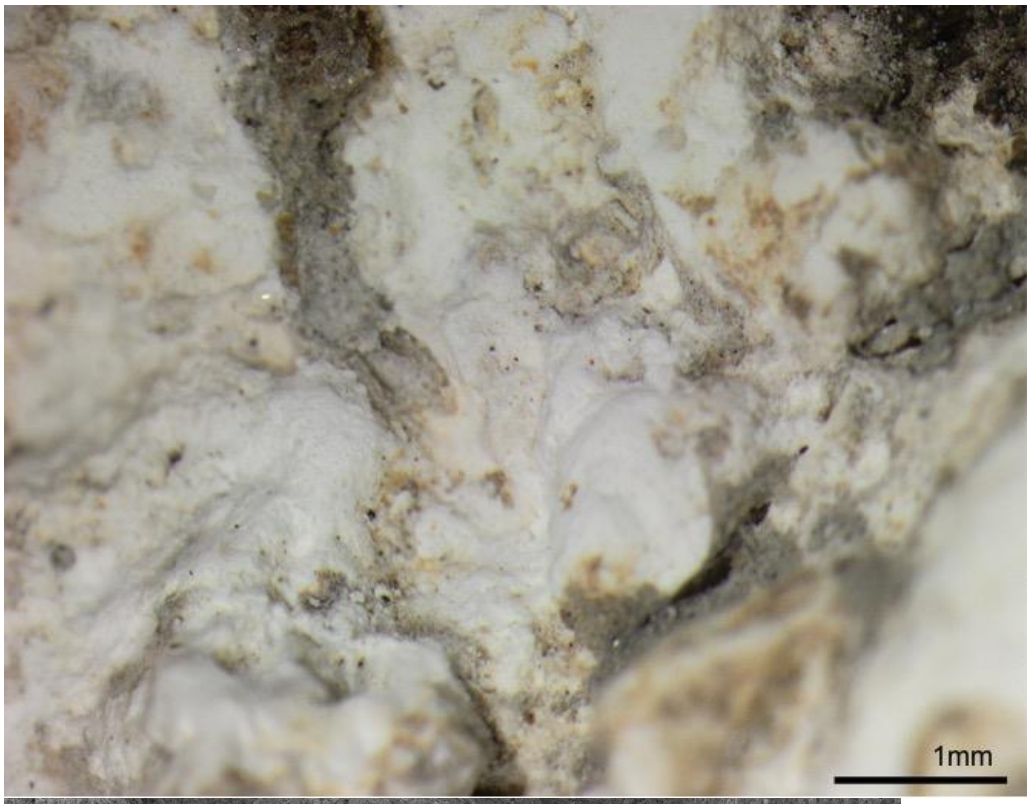

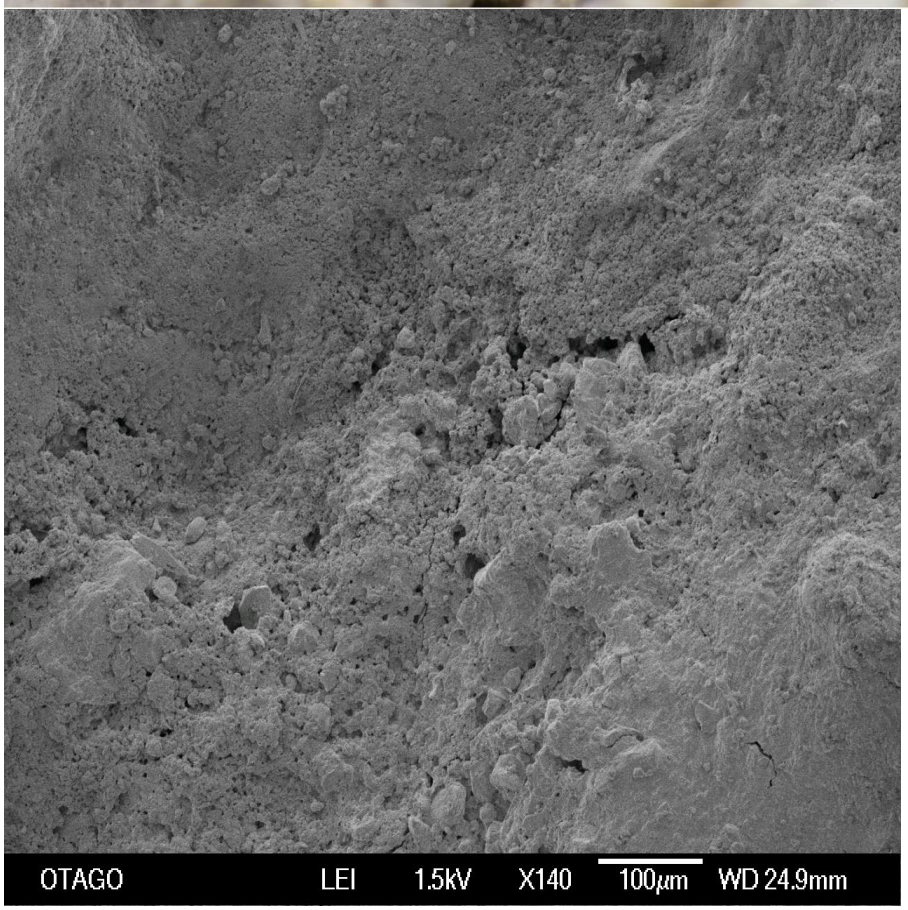

Figure 5.3. The inner surface of the probable cyst when seen with the naked eye and under low powered microscopy (top) and SEM (bottom) appears very chalky and highly irregular.

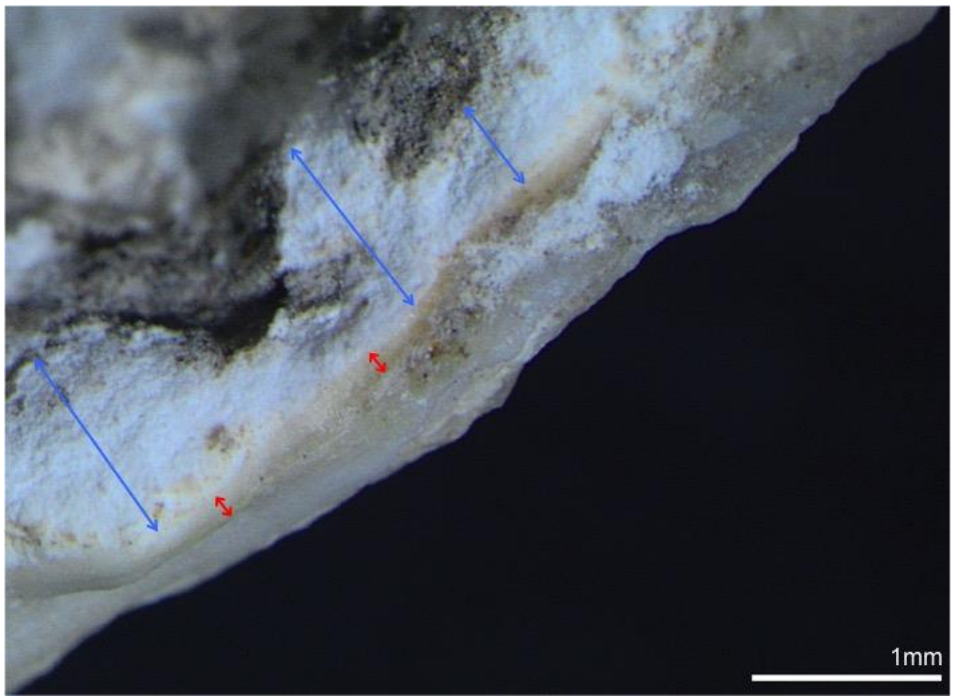

Figure S5.4. The edge of the probable cyst consists of 2 clear layers – the outer layer (indicated by the red arrows) is an average of 0.13 mm thick and may be the pericyst, and the inner layer is between 0.6 – 1 mm thick and may be the endocyst.

Micro-CT, SEM and EDS characterisation

X-ray Microtomography (Skyscan µCT X-Ray Scanner) further characterises the internal structure of the cyst showing a fibrillary structure to the internal layer in some parts which may represent a collagenous lattice and possible remnants of septa containing daughter cysts (Figure S5.5).

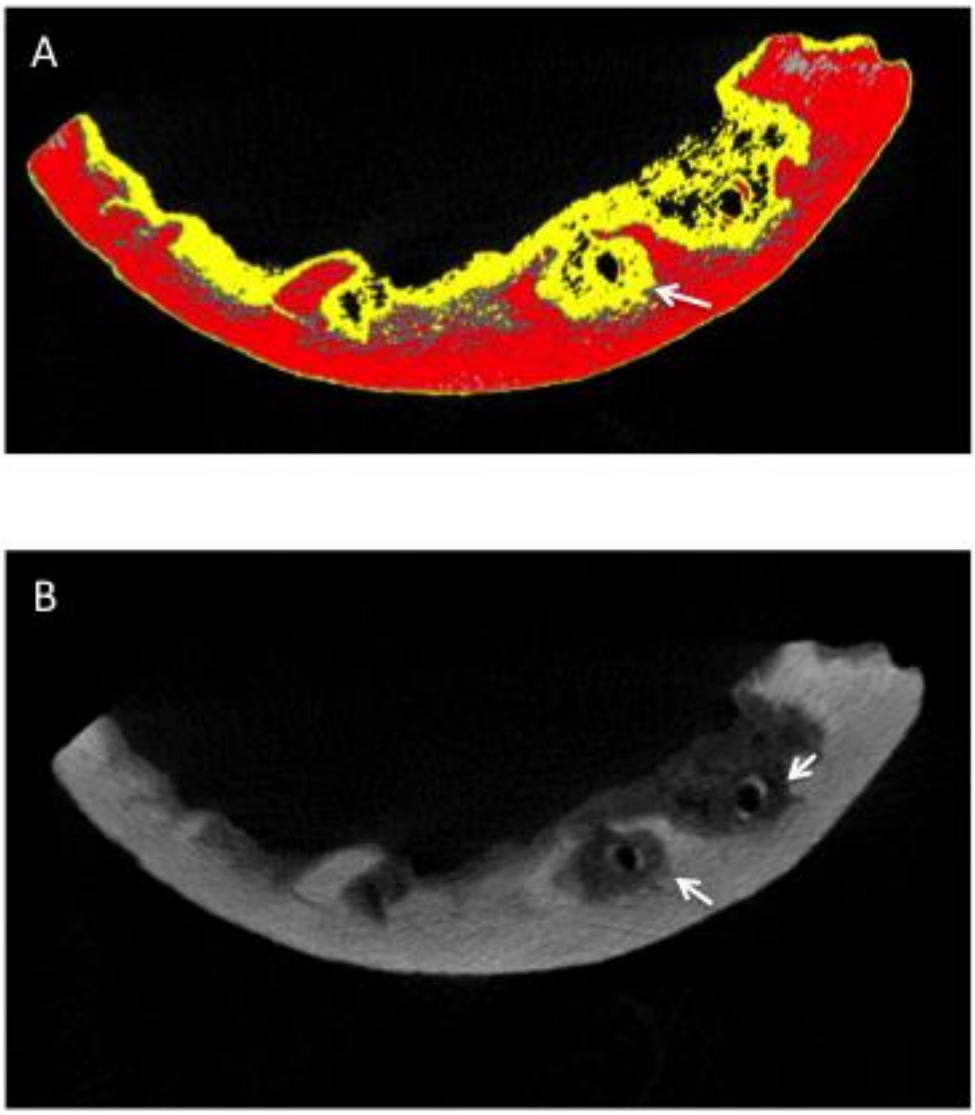

Figure S5.5: Section point through wall of cyst showing possible daughter cysts contained within septa (white arrows) associated with the inner layer. A. LUT (lookup table) of micro – CT stacks through the cyst wall shows clear division of the inner and outer layers. Red indicates the outer wall of the pericyst with possible septa remnants and yellow indicates the inner wall. The different colours denote different changes in density between the two layers. B. A greyscale version of A showing different densities.

Scanning Electron Microscopy (SEM) and Energy Dispersive X-ray Spectroscopy (X-EDS) analysis of the object topography chemical composition of the inner and outer surfaces indicate the inorganic components are made up primarily of calcium (Ca) and phosphate (P) all factors strongly supporting an endogenous origin of the cyst (Calleja et al. 2017) (Figure S5.6). The oxygen may represent organic material in the matrix.

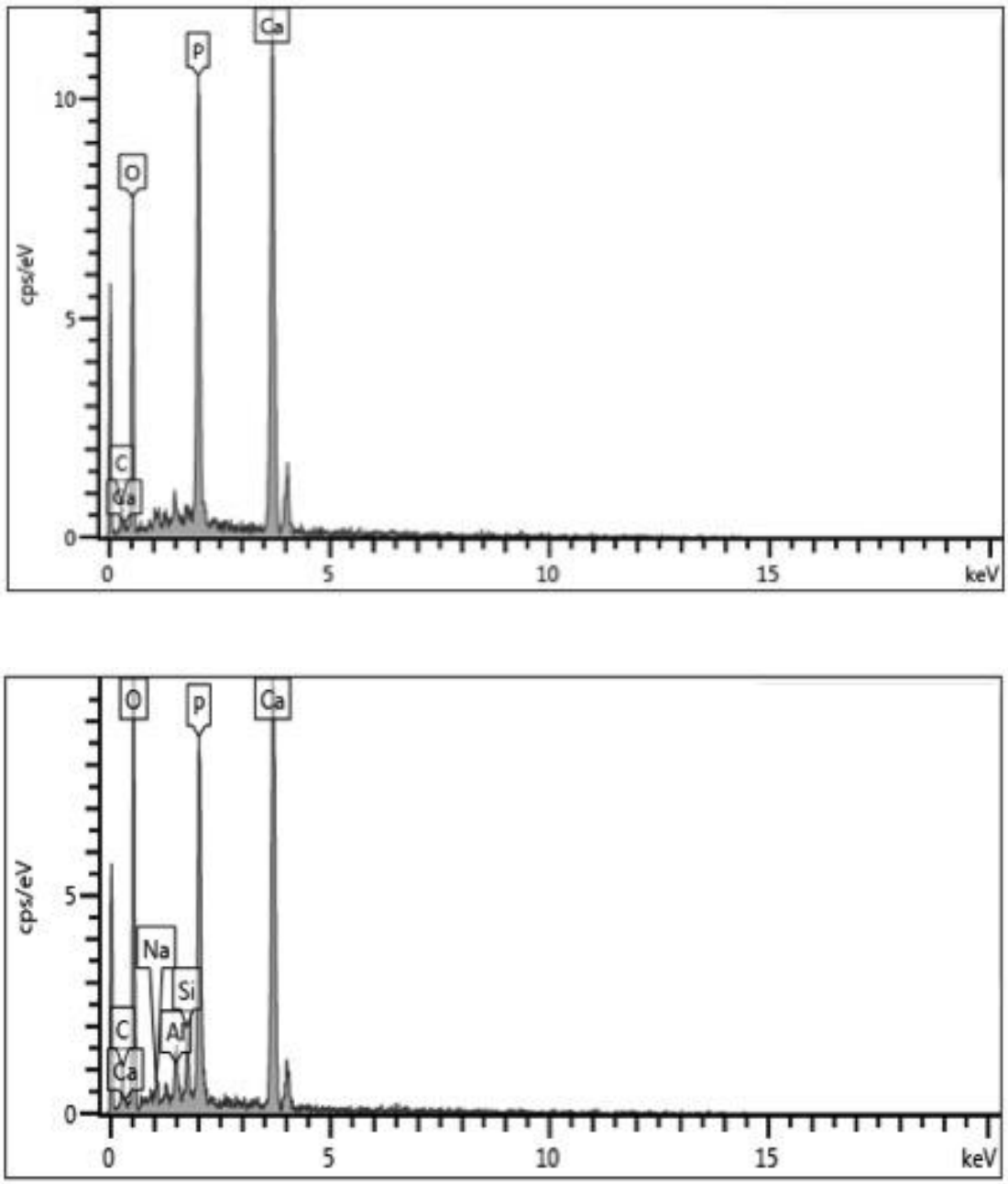

Figure S5.6. The chemical analysis of the inner surface (top) of the probable cyst consists of oxygen (45%), calcium (38%) and phosphorous (17%); the ratio of calcium to phosphate is 2.2:1. The chemical analysis of the outer surface (bottom) of the probable cyst consists primarily of oxygen (47%), calcium (34%) and phosphorous (14%) with minor amounts of silica, aluminium and sodium likely from contaminating sediment; the ratio of calcium to phosphate is 2.4:1.

Diagnosis of the cyst

Komar and Buikstra (2003) describe the causes of various types of mineralised masses and the means for differentiating them in archaeological material. Based on these descriptions and

given the small, hollow and ellipsoid morphology of the CCN cyst, several malignant and benign aetiologies can be safely ruled out. Further, this cyst was found in the pelvic area and the sex of the M59 is male -so the range of possibilities could be reduced to idiopathic intrapelvic calcification (non-ovarian due to male sex) or a possible hydatid cyst. However, as this burial was seated rather than lying flat, the source of the cyst could be from any visceral organ, including the lungs. Calleja et al. (2017) also present an exhaustive differential diagnosis of calcified cysts which is outside the scope of the current description. However, the dual layers of the cyst wall and the lack vascularisation present in the CCN cyst likely represent the asexual life cycle of a parasite than tumor genesis (Komar & Buikstra 2003).

These features taken together strongly suggest this object is a cyst formed by the Echinococcus parasite or tapeworm causing hydatids disease (Moro & Schantz 2009). One fragment has a shoulder or saddle-like formation to it that may indicate the formation of a daughter cyst characteristic of *Echinococcus granulosus* (cystic *Echinococcus)* and further septa remnants are visible macroscopically on the internal surface and possible daughter cysts are visualised in the section points of Micro CT; all features further supporting this conclusion (Waters-Rist et al. 2014).

The genus Echinococcus of cestode parasites is part of the family Taeniidae, which includes tapeworms such as Taenia saginata. The life cycles of Echinococcus species always involve a definitive host harboring the adult worm, and an intermediate host carrying the larva or metacestode. The (carnivore, usually a canid) definitive host becomes infected by ingesting protoscoleces contained within the bladder-like metacestode lodged in intermediate host viscera. Protoscoleces develop into 3-mm-long gut- dwelling adult tapeworms, which produce eggs. The intermediate host (ungulate and sometimes human) acquires infection through the accidental ingestion of eggs passed out with the faeces of the definitive host. Infection by larval Echinococcus is termed hydatid disease (Díaz et al. 2011). Transmission of the parasite between the definitive and intermediate host usually occurs through carnivore ingestion by eating of viscera containing cysts from the intermediate host. Humans can also become infected by eating of infected viscera or through close association with the carnivore and their faeces (eggs are often found around the anus, muzzle and paws of canids). In the absence of an intimate relation between ungulates and carnivores as characterised by pastoralism as at CCN, infection can occur through sharing a common water source (Moro & Schantz 2009). There are several strains of *Echinococcus granulosus* found throughout the world, mostly in temperate zones. The Sheep strain (G1) is the most widespread but the

cervid strain or northern sylvatic (G8) is maintained in cycles associated with wolves, dogs, and moose and reindeer in North America and Eurasia. This cervid strain may be the more likely cause of hydatids disease in the CCN population and is also implicated in an archaeological case from Neolithic Siberia (Waters-Rist et al. 2014). Interestingly, it is characterised by mostly pulmonary disease and is clinically less important that other strains (Moro & Schantz 2009).

An hydatid cyst is constructed of three layers; the endocyst is formed of the germinate and laminate layers on the internal aspect produced by the parasite, the exocyst superficial to these layers represent the human granuloma reaction to the pathogen, and the pericyst which is the most external layer combining the endocyst and exocyst forming a completely acellular outer layer (Brunetti et al. 2010, Díaz et al. 2011). The highly irregular morphology of the inner surface may also represent the remnants of septa associated with daughter cysts or multiplication within the endocyst.

The EDS results from the cyst outer layer are in keeping with a combined calcium phosphate matrix likely formed *in vivo* in a composition such as that expected of the pericyst (Calleja et al. 2017). While calcification of cysts is not restricted to later stages of parasite maturation, calcification is more likely as the infection progresses. Due to the post-mortem fragmentation, it is not possible to discern whether the cyst had ruptured *in vivo* resulting in anaphalaxis and death of the individual. Unless cyst rupture occurs, the presence of the hydatid cyst is usually asymptomatic. The osteolytic lesion of the right distal humeral epiphysis and large multiloculated area of lysis and fibrosis in the metaphysis visualised through plain film radiography is suggestive of hydatids of bone and supports the diagnosis of the cyst.

Similar cysts have been found in various contexts around the world (e.g. Williams 1985, Mowlavi et al. 2014, Waters-Rist et al. 2014, Antikas & Wynn-Antikas 2016) and the morphology shown by the various imaging techniques and chemical composition mirror that described by Calleja et al. (2017) for a possible *Echinococcus granulosus* cyst in a medieval female Spanish burial.

References

Antikas, T.G. & L.K. Wynn-Antikas. 2016. Hydatidosis of a Pregnant Woman of the 3rd Century Bc, Greece. *International Journal of Osteoarchaeology* 26: 920-924. https://doi.org/10.1002/oa.2475

Brunetti, E., P. Kern & D.A. Vuitton. 2010. Expert Consensus for the Diagnosis and Treatment of Cystic and Alveolar Echinococcosis in Humans. *Acta Tropica* 114: 1-16. https://doi.org/10.1016/j.actatropica.2009.11.001

Calleja, Á.M.M., N. Sarkic, J.H. López, W.D.T. Antunes, M.F.C. Pereira, A.P.A.d. Matos & A.L. Santos. 2017. A Possible Echinococcus Granulosus Calcified Cyst Found in a Medieval Adult Female from the Churchyard of Santo Domingo De Silos (Prádena Del Rincón, Madrid, Spain). *International Journal of Paleopathology* 16: 5-13. https://doi.org/10.1016/j.ijpp.2017.01.005

Díaz, A., C. Casaravilla, F. Irigoín, G. Lin, J.O. Previato & F. Ferreira. 2011. Understanding the Laminated Layer of Larval Echinococcus I: Structure. *Trends in Parasitology* 27: 204-213. https://doi.org/10.1016/j.pt.2010.12.012

Komar, D. & J.E. Buikstra. 2003. Differential Diagnosis of a Prehistoric Biological Object from the Koster (Illinois) Site. *International Journal of Osteoarchaeology* 13: 157-164. https://doi.org/10.1002/oa.670

Moro, P. & P.M. Schantz. 2009. Echinococcosis: A Review. *International Journal of Infectious Diseases* 13: 125-133. https://doi.org/10.1016/j.ijid.2008.03.037

Mowlavi, G., S. Kacki, J. Dupouy-Camet, I. Mobedi, M. Makki, M.F. Harandi & S.R. Naddaf. 2014. Probable Hepatic Capillariosis and Hydatidosis in an Adolescent from the Late Roman Period Buried in Amiens (France). *Parasite* 21: 9. https://doi.org/10.1051/parasite/2014010

Waters-Rist, A.L., K. Faccia, A. Lieverse, V.I. Bazaliiskii, M.A. Katzenberg & R.J. Losey. 2014. Multicomponent Analyses of a Hydatid Cyst from an Early Neolithic Hunter–Fisher–Gatherer from Lake Baikal, Siberia. *Journal Of Archaeological Science* 50: 51-62. https://doi.org/10.1016/j.jas.2014.06.015

Williams, J.A. 1985. Evidence of Hydatid Disease in a Plains Woodland Burial. *Plains Anthropologist* 30: 25-28. https://doi.org/10.1080/2052546.1985.11909263